A Semi-Supervised Reservoir Computing System Based on Tapered Whisker for Mobile Robot Terrain Identification and Roughness Estimation

Zhenhua Yu [1], S.M.Hadi Sadati [2], Helmut Hauser[3], Peter R.N. Childs [1],Thrishantha Nanayakkara[1]

***Abstract*—Identifying terrain type is important for safely operating robots exploration in unstructured environments. In this letter, we firstly proposed a novel tapered whisker-based semi-supervised reservoir computing (TWSSRC) system for improving terrain classification and terrain property estimation for traversability assessment with low computing cost. Three Hall sensors are used to capture the vibration at different locations of the tapered whisker. It could provide morphological computation power to achieve frequency separation in the time domain simultaneously without any data procession and only with the help of an additional simple linear regression, different signals can be classified. The movement of the robot on different types of terrain will result in different vibration behaviors of the whiskers and the whiskered robot can learn from prior physical experiences through cost-efficient self-supervised reservoir computing to achieve auto-labeling of new terrain and terrain classification. Experimental results demonstrate that this method can achieve good performance when the robot encounters new terrain and can accurately estimate the property of the unknown terrain surface at different robot speeds.**

***Index Terms*—Robotic whiskers, Semi-supervised Reservoir computing, Terrain classification, Terrain roughness estimation.**

I. INTRODUCTION

To prevent autonomous robots from losing mobility in unstructured environments and to improve traversal efficiency, robots must maintain the ability to identify the local terrain. With real-time terrain recognition, the robot can avoid hazardous obstacles, re-route safely and adapt its motion control strategy to different terrains. Therefore, the robot should to be able to actively sense the terrain quickly and accurately, preferably at the lowest computational cost to accommodate real-time applications [1].

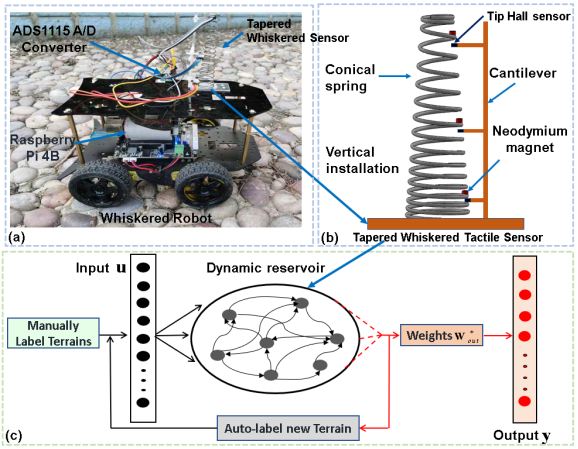

Fig. 1. Schematic of a tapered whisker-based semi-supervised reservoir computing system.(a) Whiskered Robot setup. (b) Tapered whisker sensor design. (c) Semi-supervised reservoir computing system, showing the internal reservoir, auto-label new terrain, and a readout function. The tapered shape of the spring causes different vibration frequency components to localise along the whisker when there is a vertical vibration stimuli input. In this experiment, the nonlinear tapered whisker sensor would serve as the dynamical reservoir, and only the outputs weight matrix W_{out} needs to be trained via logistic regression. Actually, there can be any number of readouts from the whisker sensor. In this particular application of terrain classification and roughness estimation, only 3 readouts could achieve sufficient accuracy.

Based on sensing modalities, robot terrain classification methods are divided into two categories: exteroceptive and proprioceptive [2]. Exteroceptive sensors, such as vision [3] [4], and lidar [5] sense the terrain from a distance, allowing a robot to identify its surroundings without direct interaction. However, these methods are susceptible to lighting conditions reducing accuracy (e.g., smoke, fog) and can be easily deceived by terrain cover (e.g., fallen leaves, snow). In contrast, proprioceptive sensor based methods, such accelerometer [6], acoustic [7], and tactile sensors [8] classify the terrain through the robot's interactive contact with the external environment. However, most state-of-the-art methods require large manually assigned labels for the training data, which is challenging for practical robotic applications in unstructured environments, such as the rovers in Mars. Therefore, self-supervised methods are proposed.

For example, Sofman proposed a self-supervised online learning method that relies on satellite images to build traversability cost maps for outdoor off-road robots [9]. Multi-modal sensor data fusion based self-supervised learning meth-

*Manuscript received: October 11, 2021; Revised: February 4, 2021; Accepted: March 3, 2022.

This paper was recommended for publication by Editor Cho, Kyu-Jin upon evaluation of the Associate Editor and Reviewers' comments. This work was supported in part by the EU Project NI "Natural Intelligence for Robotic Monitoring of Habitats" under Grant Agreement 101016970, UK Engineering and Physical Sciences Research Council (EPSRC) RoboPatient project under Grant EP/T00603X/1, MOTION project under Grant EP/N03211X/2, EP/N029003/1, Circular Construction In Regenerative Cities (CIRCuIT) ID: 821201, and in part by China Scholarship Council, and by core funding from the Wellcome/EPSRC Centre for Medical Engineering, Wellcome Trust [WT203148/Z/16/Z]. *Corresponding author: Zhenhua Yu*

[1]Zhenhua Yu, P.Childs, and T.Nanayakkara are with Dyson School of Design Engineering, Imperial College London, SW7 2DB, London, UK (e-mail:z.yu18@imperial.ac.uk,u.perera@imperial.ac.uk, p.childs@imperial.ac.uk, t.nanayakkara@imperial.ac.uk)

[2] S.M.H. Sadati is with the Department of Surgical and Interventional Engineering, King's College London, London WC2R 2LS, U.K

[3] Helmut Hauser is with the Department of Engineering Mathematics, University of Bristol, Bristol BS8 1TH,U.K,and also with the SoftLab, Bristol Robotics Laboratory, U.K.(e-mail:helmut.hauser@bristol.ac.uk)

Digital Object Identifier (DOI): see top of this page.

ods have been investigated [10] [11]. One of the challenges for this approach is that it requires large computing resources for data processing and learning model training.

An alternative approach to achieve self-supervised online learning with low computational cost is to use physical reservoir computing [12]. This utilizes the complex dynamics of the physical body as a computational resource, and therefore it could significantly reduce the required computational power. This method is based on a machine learning approach which is called reservoir computing [13], and it can be used to quickly learn the dynamic input-output relationships. At its core is a nonlinear, high-dimensional dynamical system (i.e., the *reservoir*) that maps any input nonlinearly signals into its high-dimensional state space, while integrating temporal information with a leaked memory, as shown in Fig.1. If the dynamics of the reservoir is sufficiently complex, then adding a simple linear readout is sufficient to simulate a complex nonlinear dynamical system [12]. It means that the complex computations can be reduced to finding a set of linear output weights just through using simple linear regression with the help of the nonlinear dynamics of reservoir learning. Even though the reservoir computing is an abstract machine learning method, *physical reservoir computing* uses real physical systems as reservoirs. This includes networks of memristors, nonlinear effects in lasers, compliant body parts of robots and may others [14].

We proposed a semi-supervised reservoir computing system that for the first time uses a tapered spring as the reservoir mounted on a mobile robot for terrain classification and surfaces property estimation (Fig.1), inspired by the rapid movement of rats using their whiskers in a dark and unfamiliar environment. We were inspired by the fact that the movement of the robot over different types of terrain would result in different vibrational behavior of the tapered spring. The readout from the tapered whisker reservoir is achieved by means of a Hall effect sensor to read the voltage changes due to the vibration of three magnets located at the bottom, middle and top of the spring. In our previous research, Hauser et al. [15] has demonstrated that a compliant mass-spring systems network can be used to emulate complex nonlinear systems such as the controller, filters, limit cycles. In this paper, only use one tapered spring, it allows us to access different frequency components simultaneously. This paper firstly shows that the state response of nonlinear vibration dynamics of tapered whisker can be used to auto-label new terrain and estimate the surfaces properties of the unknown terrains based on prior physical experiences through cost-efficient self-supervised reservoir computing.

This paper is organized as follows: Section II demonstrates the design and construction of tapered spring-based whisker and the experiment data collection. The whisker based reservoir computing and how it is used for unknown terrain surfaces property prediction are studied in Section III. Section IV reports the algorithm framework of the semi-supervised reservoir computing system. Section V presents the semi-supervised reservoir computing based terrain identification experiments results, as well as the terrain properties estimation for an unknown terrain. Section VI concludes this paper's contribution as well as discusses future work.

II. Sensor and System design

A. Tapered Spring-based Whisker Sensor Design

In this letter, the phenomena of vibration frequency separation along the axis of a tapered spring is used, and it was installed vertically on the front of the mobile robot [16]. The suggested nonlinear tapered whisker-based sensor is detailed shown in Fig.1, as well as the four-wheeled mobile robot employed in the experiment. A high carbon tapered nonlinear spring serves as the physical reservoir, and the bottom, center, and top of the tapered spring beam are all implanted with three three neodymium permanent magnets. To observe the oscillations caused by mobility across different terrains, three SS49E linear Hall sensors were mounted orthogonally by the cantilevered beam beneath the neodymium permanent magnets.

As the robot traverses different terrains in a steady state, external vibrations act vertically on the tapered whisker spring axis, resulting in a nonlinear vertical displacement along the tapered spring axis which will be used for terrain classification. Even though the robot itself has various types of vibration when it traversing different terrains, these vibrations due to external terrain stimuli does not have a significant effect on our classification results. This is because the dominant frequency of sensor is exactly same as the base vertical perturbation excitation frequency of the mobile robot caused by the external stimuli and the profile amplitude (i.e ground profile height) is the dominant factor in affecting the whisker sensor displacement as well as the sensitivity of the whisker sensor. We have demonstrated these through the theoretical model analysis as well as practical experiments in our previous research [17].

B. Reservoir Feature for Terrain Identification

To achieve cost-efficient terrain identification, n time-series vibration voltage points are sampled from the Hall sensors at the top (T), middle (M), and bottom (B) of the tapered whisker. The jth data point is denoted as $d_j^T,\ d_j^M,\ d_j^{\mathrm{B}}$, $j = 1, 2, 3, \cdots, n$ for top, middle, and bottom respectively. A sampling frequency of $f_{samp} = 100$Hz was used. Sampled data were then grouped into $n \times 3$ sampling segmented vector $D^{n\times 3}$. The jth row of $D^{n\times 3}$ is given by

$$D_j^{1\times 3} = \left[\begin{array}{ccc} d_j^T & d_j^M & d_j^B \end{array}\right] \quad j = 1, 2....n, \tag{1}$$

where each matrix row means the three streams of Hall effect sensor voltage outputs at a given time j.

The covariance matrix C_D of the segmented vibration vector $D_j^{n\times 3}$ was calculated and then decomposed into its Eigen representation for subsequent fast logistic regression training as follows:

$$C_D = cov_{p,q} = R_{vec} R_{val} R_{vec}^T \quad p, q = T,\ B,\ M, \tag{2}$$

Finally, a reservoir feature vector R_f which work as the inputs for logistic regression training is given by:

$$R_f = [R_{vec} \quad R_{val}]^T \tag{3}$$

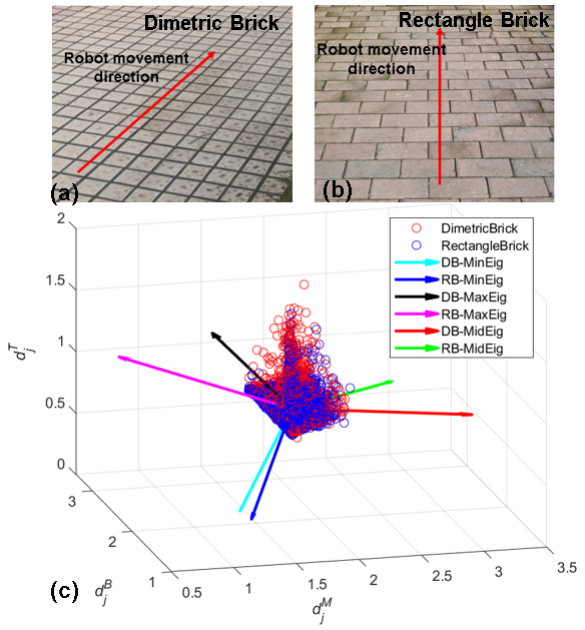

Fig. 2. The three streams Hall effect sensor voltage outputs d_j^T, d_j^M, d_j^B of two similar terrain surfaces along with the three associated Eigenvector directions and Eigenvalue scaling (RB represents Rectangle Brick and DB represents Dimetric Brick) . This demonstrates the proposed semi-supervised reservoir computing system could discriminate even two very similar terrain surface based on the whisker reservoir outputs.

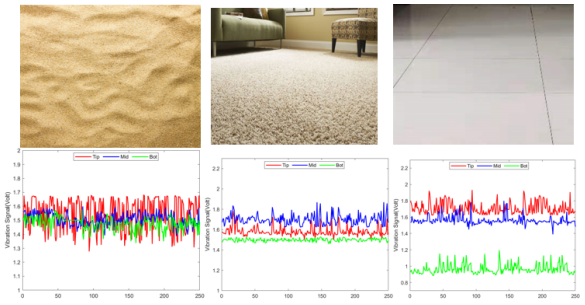

Fig. 3. Three terrain surfaces along with the associated three streams vibration signal, which is used to evaluate the performance of our RC system. (a) Soft roughish sand. (b) Soft smooth carpet. (c) Hard smooth flat tile.

Reservoir computing normally requires a high-dimensional state space with a large readout, but to fit the application of terrain classification in this study, we reduce the readouts and chose a restricted readout only with 3 here from a larger reservoir occuring in the tapering spring. As shown in Fig.2, by relying on just 3 outputs, we can distinguish two very similar brick terrains. In fact, the whisker sensor may provide an endless number of terrain recognition readouts.

C. Dataset collection

During the experiments, the whiskered robot moved at a steady speed of $0.2m/s$ traversing six different types of terrains with different hardness and roughness to test the performance of our proposed TWSSRC system as well as its capability in estimating the surface properties of new unknown terrain. Part of the sampled experiment terrain surface and its corresponding three streams vibration data are given in Fig.3. Two of these were indoor surfaces and four were outdoor terrains:

(1). hard rough cobblestones, (2). hard roughish brick
(3). soft rough grass, (4). soft roughish sand
(5). hard smooth flat, (6). soft smooth carpet

The sampling frequency of the whisker sensor was 100 Hz, and the collected data was segmented into single training feature vectors with a time window $T = 1.5$ seconds for later processing. In total, 600 seconds of vibration data from our system were originally collected for each terrain surface, which finally constructed our dataset $\mathbf{D}_i^{n\times 3}$ to evaluate the performance of the semi-supervised reservoir computing system.

III. Unknown Terrains Surfaces Properties Prediction

A. Reservoir Computing Based Terrain Classification

A dynamical tapered whisker could provide morphological computation power for projecting features from the external temporal vibration data for model training. Therefore, the reservoir computing only requires a simple logistic regression to train the output weight matrix W_{out}^T which connects the reservoir state $x(t)$ and the output $y(t)$ as shown in Fig.1.

The inputs of reservoir computing system are the reservoir feature vector R_f, which will be imported to train the logistic regression network, to get the highest probability $g(\alpha)$ of the expected possible terrain surfaces.

As shown in Equation 4 and 5, the probability of the expected possible terrain surfaces is determined both by the input reservoir feature vector R_f and the LR weight matrix W_{out}.

The value of $g(\alpha)$ will be given by a sigmoid function:

$$g(\alpha) = \frac{1}{1+e^{-\alpha}} \tag{4}$$

where $\alpha = W_{\text{out}}^T \cdot R_f$ is expected output for the reservoir feature vector R_f and it results in

$$h = g(W_{\text{out}}^T \cdot R_f) \tag{5}$$

B. New Unknown Terrain Detection

The purpose of the new unknown terrain detection stage is to predict whether a newly acquired terrain segment D^{new} belongs to a class in the existing training class or to a new unknown terrain class. Even though reservoir computing could provide the highest probability of terrain predictions for new terrain segment, when the new segment was collected from a new terrain class, the prediction probability it gives will be inaccurate and the result can have catastrophic impact for the robot.

As the results in Fig.2 suggested, different hardness and roughness terrains surfaces will result in unique eigenvalues and eigenvector direction in the Eigenspace, even though the actual topographic features of these two brick terrains are very similar. In order to detect a new unknown terrain, we introduce the Mahalanobis distance M_{D} in the Eigenspace, because it considers the synergistic influence of an eigenvector's direction

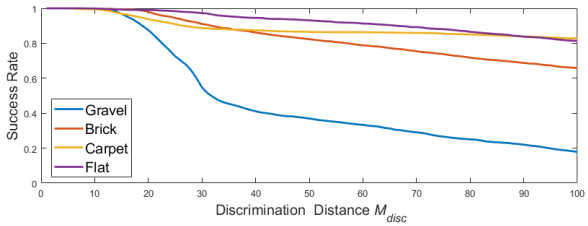

Fig. 4. The new terrain detection success rate of different unknown testing terrain datasets. Experiments were performed on several different discrimination distance M_{D} of these four testing terrains.

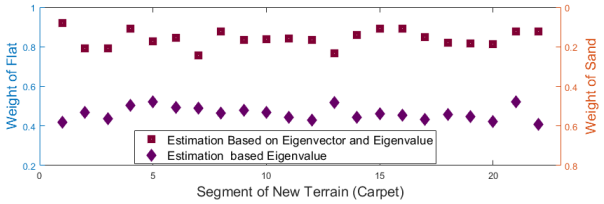

Fig. 5. New terrain estimation results with carpet working as the new terrain class, and the two nearest terrain classes are the flat surface and sand respectively.The Y-axis indicates the weight $x_{nearest\_i}$ of each terrain class.A larger weight value $x_{nearest\_i}$ means that the unknown terrain is closer to the properties of the corresponding terrain.

and eigenvalues scale which reflects the the terrain surface properties. Its mathematical expression can be expressed as

$$M_{\mathrm{D}} = \sqrt{(\hat{\mathbf{R}}_f - \mathbf{R}_f)^T C_D{}^{-1} (\hat{\mathbf{R}}_f - \mathbf{R}_f)} \tag{6}$$

where $\hat{\mathbf{R}}_f$ is the reservoir features of unknown terrain and $\mathbf{R}_f$ is the existing data reservoir feature base in Eigenspace.

To achieve accurate detection of new terrain, a novelty detector based on M_{D} is proposed in this section.

$$F(D_{new}) = \begin{cases} D_{new} = Unknown & M_D > M_{disc} \\ D_{new} = Prediction & M_D <= M_{disc} \end{cases} \tag{7}$$

where M_{disc} is the discrimination distance chosen by us. This will be employed to determine if the segment D^{new} belongs to the specified terrain class, as shown in the Equation 7. When the distance M_D is greater than the discrimination distance M_{disc}, this model will recognise it as a new unknown terrain. In contrast, the terrain class for this segment is determined the results given by the reservoir computing.

Fig.4 shows the new terrain detection success rate of different M_{disc}, with the gravel, brick, carpet, and flat surface working as the new unknown terrain class respectively. From the Fig.4, we can see that there is a 94.6% average success rate to separate each unknown terrain type from the existing terrain dataset when $M_{disc} = 20$. With the same M_{disc}, Gravel has the smallest detection success rate, but still has a 87.56% probability of distinguishing it from known databases . Therefore, the discrimination distance M_{disc} will be an important influence and optimization index for the model, which will affect the consumption of computational resources and the speed of novelty decisions. Finally, a novelty detector combining the discrimination distance M_{disc} with reservoir computing prediction result is proposed in the semi-supervised reservoir computing system to achieve fast and accurate terrain identification.

C. Terrain Properties Prediction

When a new terrain class D^{new} is identified, its physical properties are unknown because there is no corresponding extrinsic label to accurately indicate its attributes. In order for the robot to accurately self-assess whether the terrain is traversable in an unstructured environment, our semi-supervised reservoir computing system attempts to assign the texture attributes to this new terrain with good enough accuracy based on the existing terrain property database.

Temporal features extracted from a vehicle accelerometer, such as the mean, variance, and skewness, have been used for terrain classification [8]. The variance of the acceleration signal is a good indicator of the vertical motion of the robot as it moves over different terrains. However, the acceleration features are indistinguishable for different smooth surfaces [18]. For two different surfaces with the same unevenness, but different material, the variance of their accelerations may be the same, but the impact on whether the robot can traverse is quite different, e.g., the soft sand and grass.

To accurately estimate the physical properties of the new terrain D^{new} based on our TWSSRC system, we first need to identify the two closest terrain classes $D^{nearest\_1}$, $D^{nearest\_2}$ to the new terrain in the Eigenspace based on the Mahalanobis distance M_D. At the same time, we introduce the eigen coefficients $x_{nearest\_i}$ in this paper to accurately demonstrate the new terrain properties based on prior-known information. The value of the $x_{nearest\_i}$ is determined by the Mahalanobis distance M_D between the new terrain D^{new} and the corresponding two nearest terrains $D^{nearest\_1}$, $D^{nearest\_2}$ classes. An arithmetic example to calculate the eigen coefficients $x_{nearest\_1}$ based on the nearest terrain classes' reservoir feature vectors $\mathbf{R}_f^{nearest\_1}$, $\mathbf{R}_f^{nearest\_2}$.

$$x_{nearest\_1} = \frac{M_D(R_f^{new}, \mathbf{R}^{neares\_1})}{M_D(\mathbf{R}^{neares\_1}, \mathbf{R}^{neares\_2})} \tag{8}$$

The advantage of using the Mahalanobis distance M_D of the reservoir features $\mathbf{R}_f$ is that it takes into account both the direction of the eigenvector R_{vec} and the scaling of the eigenvalues $\mathbf{R}_{val}$. If we rely only on the scaling of the eigenvalues $\mathbf{R}_{val}$, whichs reflect the dispersion of the original data in a certain direction, this will result in inaccurate estimates of terrain properties, just as if we relied only on the variance of the acceleration.

Therefore, the new terrain class D^{new} could be represented as a weighted sum of existing known terrain, e.g., half carpet and half grass. Its mathematical expression is:

$$D^{new} = x_{nearest\_1} \cdot D^{nearest\_1} + x_{nearest\_2} \cdot D^{nearest\_2} \tag{9}$$

where $x_{nearest\_1}$ and $x_{nearest\_2}$ are the weight value of these two nearest terrain classes $D^{nearest\_1}$ and $D^{nearest\_2}$.

Fig.5 shows the terrain estimation results when we use carpet as the new terrain class based on Equation.8. It can be seen from the square point in Fig.5 that the new carpet terrain could be represented as

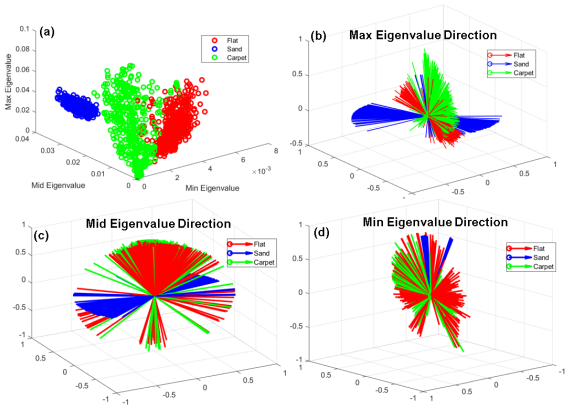

Fig. 6. The three Eigenvalue scaling and its associated Eigenvector directions of the carpet, flat surface and sand respectively. This demonstrates that the carpet is much more similar with the flat surface.

$$\text{Carpet} = 0.8415 \cdot \text{Flat} + 0.1585 \cdot \text{Sand} \quad , \qquad (10)$$

which means that the carpet properties are closer to the flat surface than to sand. In contrast, if we rely only on the magnitude of the eigenvalues, we will get the result as shown in the purple square in Fig.5 which means carpet will be represented by half sand and half carpet.

We believe that the weight of squares points in Fig. 5 reflect more accurately than the diamonds for the new terrain characteristics. This is because the eigenvalue orientation of the carpet is generally more similar and close to that of the flat surface, rather than being in the middle of the sand and the flat, as shown in Fig.6. It is important to note that the orientations of the eigenvalues show the characteristics of the whisker reservoir output values due to different external excitations. In addition, through manual observation of the three terrains, the smoothness of the carpet and the floor is closer in our experiment as shown in Fig.3, but the carpet will also be a little soft similar to the soft sand.

IV. Semi-supervised Reservoir Computing

In this section, we will describe how to employ TWSSRC for auto terrain identification, including the properties prediction of an unknown terrain, the auto-label of the new terrain class and terrain classification.

A. Reservoir Computing Based Terrain Prediction

As shown in Fig.7, the terrain classification begins with the acquisition of a terrain segment signal by the robot. The whiskered robot could receive the maximum possible terrain prediction as well as its corresponding prediction probability based on the tapered whisker-based reservoir computing described in Section III-A, which will be used for the later novelty detection for new terrain class.

B. New Terrain Detection

The target of the *novelty decision model* (see Section III-B) is to decide whether a newly acquired terrain segment D^{new} belongs to a class in the existing training set or to a new unknown terrain class. Without the novelty detection, the new unknown terrain signals would be classified wrongly which might lead to catastrophic consequences for the robots. The *novelty decision model* will firstly decide whether it need to calculate the M_{D} between the new terrain segment D^{new} and the existing terrain dataset considering the prediction probability from reservoir computing.

The *novelty decision model* will then assess whether this new terrain is a known terrain (rejected) or an unknown terrain (accepted) in the following stage, depending on the information M_{D} provided. In the event of rejection, the mobile robot will use the reservoir computing results to determine the terrain type of the new segment, and the terrain segment D^{new} will be saved for subsequent model training.

If the new terrain segment D^{new} is "accepted", its texture properties are unknown due to there is no corresponding extrinsic labels to accurately indicate its attributes. Therefore, our semi-supervised reservoir computing system attempts to assign the attributes to this new terrain with relative accuracy based on the existing terrain property database using the methods described in Section III-C.

C. Create and Auto-label New Terrain Class

Before adding a new terrain category to the prior known terrain database, we must collect a sufficient number segments of the new terrain. During the experiments in this paper, we set this data criterion to 30 segments. Until this number is reached, all new terrain data will be stored in a temporary buffer. To avoid outliers of known terrain categories being misclassified as new terrain categories, they are added to the terrain database only when two consecutive data are judged to be the same terrain.

Whenever a new terrain has more than 30 segments data stored in the buffer, we create a new terrain class and add it to the database of known terrains. At the same time, based on the method described in Section III-C, we will assign terrain properties to this new terrain and label it automatically.

D. Update of a Known Class

To save computational resources, the system does not update the terrain database in real time, but updates the entire known terrain database only after the new segment number of a certain new terrain reaches 20. This is because we must recompute the LR weight matrix W_{out} and the reservoir feature database $\mathbf{R}_f$ simultaneously each time when the training data is updating. At present, our system has a fixed number $N = 200$ of each terrain category, but more training data will improve the accuracy of recognition.

In order to avoid LR weight matrix W_{out} retraining misalignment due to uneven distribution of training data, the new terrain class will not be added to the prior known training database until the new class reaches the fixed number $N = 200$ to ensure the data balance.

V. Experiments Results

Terrain classification and surface properties estimation of unknown terrain experiments using the TWSSRC system were

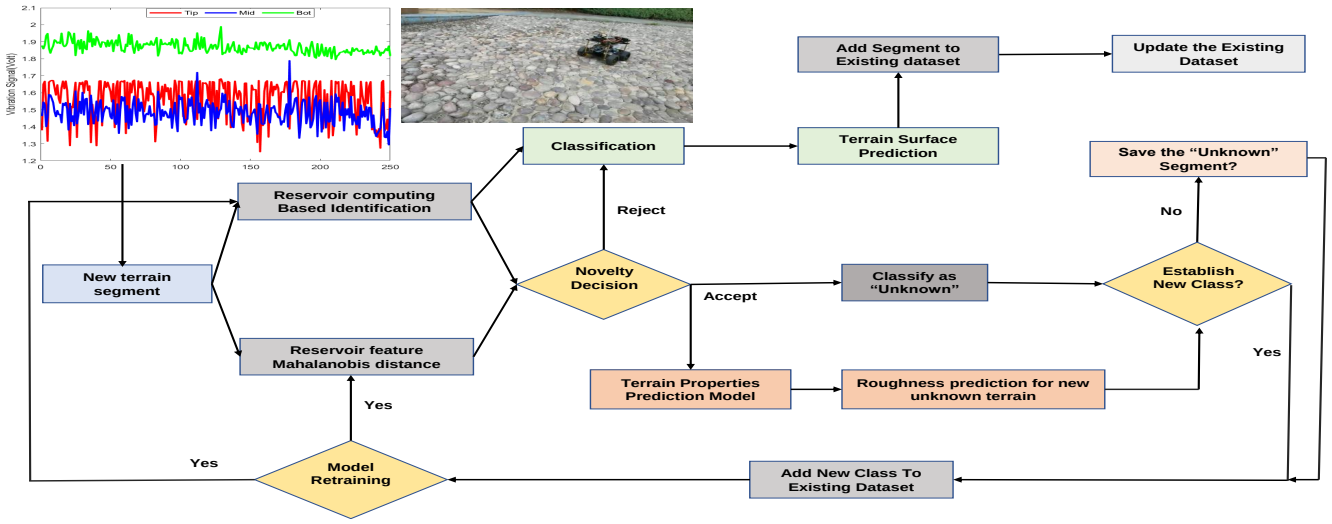

Fig. 7. The workflow of Semi-supervised Reservoir Computing system based on the tapered whisker tactile sensor. The robot could add the new unknown terrain surfaces with its texture proprieties information to existing dataset by itself and keep updating the prior-known terrain database.

TABLE I
NEW TERRAIN DETECTION SUCCESS RATE FOR DIFFERENT M_{disc}

	$M_{disc} = 17$	$M_{disc} = 23$	$M_{disc} = 29$
Existing Terrain Dataset	91.9%	89.2%	83.7%
New (Carpet)	87.3%	83.2%	79.1%

carried out on six different terrains with the mobile robot at a steady traverse speed of $0.2m/s$ to verify the robustness and reliability of the aforementioned methods.

A. Performance of New Terrain Detection

In this experiment, carpet was chosen as the new terrain class to evaluate the performance of *novelty decision model* for detecting unknown new terrain, and the test 5 terrain classes were the prior known terrain database. When the logistic regression prediction probability P_{disc} of a new segment was greater than 70%, we classified it directly based on the LR prediction result. If the logistic regression prediction probability P_{disc} of a new segment was less than 70%, the system will judge whether the segment is a new terrain or which class of terrain it belongs to based on the discrimination distance M_{disc}. Table. I showed the successful detection rate of new terrain (carpet) relative to various M_{disc}, which demonstrate that relying on a strict discrimination distance M_{disc}, we can achieve the accurate detection of new terrain.

Comparing the results in Fig.5, the main reason for the decrease in success rate here was that logistic regression model may misjudged a terrain since the probability value P_{disc} we set was too small, thus making it impossible to accurately determine the new terrain. For example, the model may misjudge a blanket as a floor based on the probabilistic results of logistic regression. Therefore, a trade-off between the differentiation distance M_{disc} and the probability value P_{disc} is needed to achieve high recognition accuracy with as few computational resources as possible.

B. Semi-supervised Terrain Identification

During the repeated random sub-sampling validation experiments to test our proposed TWSSRC system's performance

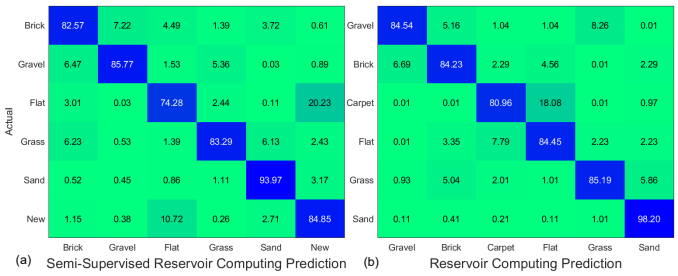

Fig. 8. (a). Confusion matrix of semi-supervised reservoir computing prediction success rate averaged over 10 randomly trials, with Carpet working as the new unknown terrain. (b). Confusion matrix of reservoir computing prediction success rate over six terrain. The robot speed is $0.2m/s$, sampling frequency of the whisker is 100Hz, $M_{disc} = 17$. and the time window size 1.5 s.

in unstructured environments, carpet was chosen as the new terrain $\mathbf{D}_{unknown}$ to simulate the robot independently identifying and predicting new terrain in unknown environments based on prior existing databases.

70% data of the priori datasets (not including the Carpet signal) $\mathbf{D}_p$ were randomly selected for the LR weight matrix training. Then the remaining 30% of data $\mathbf{D}_p$ as well as the testing unknown terrain $\mathbf{D}_{unknown}$ was used to test the performance of our proposed semi-supervised reservoir computing system. To eliminate inadvertent categorization mistakes induced by random trials, a total of 10 random tests were undertaken.

Fig.8(a) shows the identification results using our proposed semi–supervised reservoir computing system which could identify the new terrain class with a success rate of 84.85% when the discrimination distance $M_{\mathrm{D}} = 17$ and 85.59% accuracy for the prior-known datasets $\mathbf{D}_p$. In order to evaluate the performance of our proposed semi-supervised algorithm, we directly performed reservoir computing based terrain classification experiments using the data from these six terrains directly, the result is shown in Fig.8(b), which achieve 86.2% average accuracy. Comparing the results in Fig.8, it indicated that the proposed semi–supervised methods could accurately identify the new unknown terrain $\mathbf{D}_{unknown}$ and discriminate

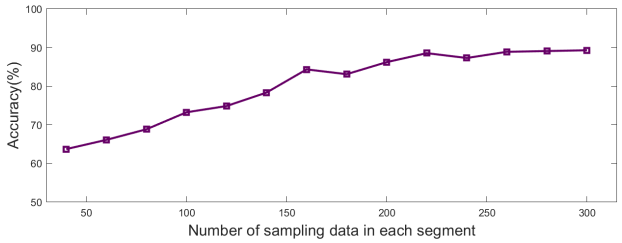

Fig. 9. Classification accuracy of our proposed semi-supervised model when trained on different numbers of data in each training segments. The accuracy increases with the number of data used for model training.

it from the already existing terrains inside the priori datasets $\mathbf{D}_p$.

However, there is a significant confusion of about 20.23% between the unknown terrain $\mathbf{D}_{unknown}$ and Flat $\mathbf{D}_{flat}$. The reason for this is that the *Novelty decision model* cannot accurately identify the new terrain, and thus many segments of new terrain are misclassified as flats. This is why our proposed semi-supervised method has a reduced classification accuracy for known terrain, compared with the supervised reservoir computing. Therefore, parameter optimization of the *novelty decision model* will become the next stage's research direction to improve the new terrain detection accuracy and a trade-off must be done between the identification accuracy and computation cost.

Deep learning approaches require a large number of training data, and they could achieve better performance when the amount of correct training data increases. We also investigated the effect of relationship between the number of data points included in each training segment and the classification accuracy of the model. Fig.9 demonstrates the results of these experiment, and it suggests that the accuracy of the model benefits from the inclusion of more data in each training segment.

C. Terrain Properties Estimation

In this section, we focus on accurate property prediction of new terrain when the robot is moving unstructured environments at a steady speed $0.2m/s$.

Fig.10 gives the predicted surface properties when we take Carpet, Brick, and Grass as unknown test terrain respectively. For Carpet and Brick, the proposed method could give relatively accurate predictions when they are used as unknown terrain, e.g. $Brick = 0.75 * Gravel + 0.25 * Flat$, which objectively reflects the properties of the new terrain. However, the estimation results for grass is not sufficiently accurate because we do not have enough known terrain data in our a priori database to describe this new terrain feature.

Overall, this terrain properties estimation method we propose based on the reservoir outputs is crucial for the robot's assessment of the traversability of unknown terrain, especially where we cannot collect sufficient training data in advance for model training, e.g., for Mars rovers.

D. Performance Evaluation Over External Disturbance

In this section, we will explore the influence of external disturbances e.g. sudden wind gust or bumps on the terrain on

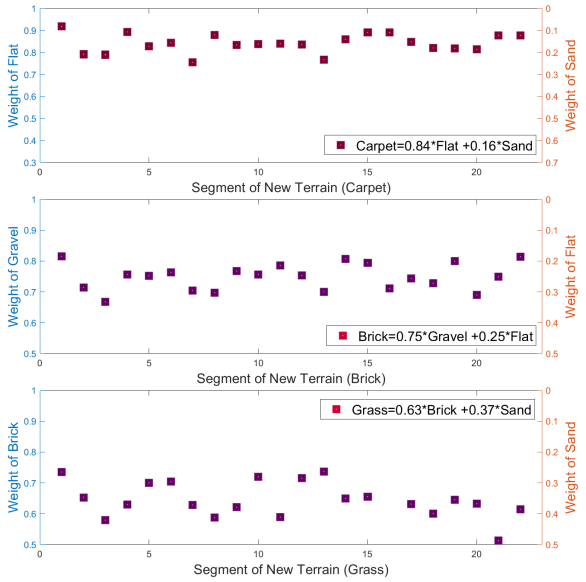

Fig. 10. New terrain properties estimation results of our semi-supervised RC based on prior existing dataset, with Carpet, Brick, and Grass as the new unknown terrain class respectively. The Y-axis indicates the weight of each terrain class. A larger weight value $x_{nearest\_i}$ means that the unknown terrain is closer to the properties of the corresponding terrain.

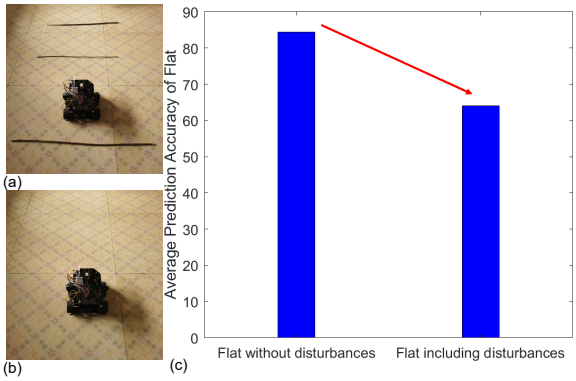

Fig. 11. (a). Thin strips of wood were placed on the flat as a disturbance. (b). Flat terrains experiment scene without disturbance. (c). Comparison of terrain classification results based on TWSSRC algorithm in these two scenarios. The recognition accuracy will drop when there is external disturbance.

our proposed TWSSRC system's performance by adding thin wood strips to the flat surface as disturbances, as shown in Fig.11 (a) and Fig.11 (b).

As shown in Fig.11 (c), when there are thin wooden strips as disturbance signals over flat, our method might discriminate the vibration signal segments containing the disturbance as a new terrain, which leads to a decrease in identification accuracy, but still identifies the terrain with about 64% accuracy. This means that if there is a sudden external disturbance, the accuracy of our algorithm will be affected to some extent.

However, the algorithm can use the largest probability assigned to a class of terrain as the most likely terrain to be robust in the presence of disturbances. It can be extended to use different probabilities assigned to different possible terrain conditions including a "new" terrain when the terrain is not homogeneous.

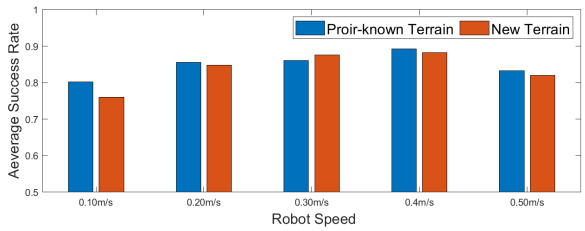

Fig. 12. Semi-supervised reservoir computing terrain identification results when the robot traversing several terrains with different steady speed, using the Carpet as the new unknown terrain class.

E. Performance Evaluation at Different Robot Speed

In this section, the influence of different speeds on our proposed TWSSRC system's performance would been explored. Data collection was performed at diverse steady speeds of 0.1 m/s, 0.2m/s, 0.3m/s, 0.4 m/s and 0.5 m/s respectively over these six terrains, and the Carpet terrain class will be used as the unknown terrain class too.

From the Fig.12, it can be seen that this system has good identification accuracy of new terrain and accurate classification results for five prior known terrains at different speeds. It is worth noting that the system achieves its best at speed $0.4m/s$, however, the recognition accuracy decreases at speeds $0.1m/s$ and $0.5m/s$. This can be explained by the fact that when the robot speed is very low, its self-vibration will have a greater effect on the whisker sensor; while when the speed is very fast, different terrain stimuli will cause chaos in the separation signal of the whisker sensor, thus degrading its performance.

In all, a mobile robot can change its speed to elicit the frequency separation of whisker sensor signal to help terrain classification.

VI. CONCLUSIONS AND DISCUSSION

A novel tapered whisker-based semi-supervised reservoir computing algorithm was proposed for the first time for new terrain identification, terrain property estimation, terrain classification and validated using a whiskered robot in a unstructured environment. This approaches can successfully detect the new terrain classes, and achieve 84.12% accuracy over six terrain with carpet representing the new terrain class. The proposed scheme could also precisely estimate the terrain properties of new terrain and auto-label it based on prior existing experience.

However, there is still a lot of work to optimize parameters such as the discrimination distance M_{disc} of this system and thus the trade-off between computational cost and identification accuracy. Another factor affecting the performance of the algorithm is external disturbances such as a sudden wind gust or bumps on the terrain, which would cause the robot to misjudge and thus affect the prediction accuracy. However, these disturbances can be addressed by a secondary disturbance observer running in parallel in our later work. Moreover, it's would be interesting to investigate the effect of driving condition, such as the drive rear and turn,on the classification performance in future work.

In all, the experiment results have shown the potential of proposed method for the terrain identification and classification of a completely unknown world without an excessive amount of human intervention and the whiskered robot could use speed control to achieve better identification performance. Besides, this method is less affected by the vibration of the robot itself, so it can be well transferred to other robots without customization.

REFERENCES

[1] K. Otsu, M. Ono, T. J. Fuchs, I. Baldwin, and T. Kubota, "Autonomous terrain classification with co-and self-training approach," *IEEE Robotics and Automation Letters*, vol. 1, no. 2, pp. 814–819, 2016.

[2] R. Gonzalez, D. Apostolopoulos, and K. Iagnemma, "Slippage and immobilization detection for planetary exploration rovers via machine learning and proprioceptive sensing," *Journal of Field Robotics*, vol. 35, no. 2, pp. 231–247, 2018.

[3] F. Schilling, X. Chen, J. Folkesson, and P. Jensfelt, "Geometric and visual terrain classification for autonomous mobile navigation," in *2017 IEEE/RSJ International Conference on Intelligent Robots and Systems (IROS)*. IEEE, 2017, pp. 2678–2684.

[4] M. Nava, J. Guzzi, R. O. Chavez-Garcia, L. M. Gambardella, and A. Giusti, "Learning long-range perception using self-supervision from short-range sensors and odometry," *IEEE Robotics and Automation Letters*, vol. 4, no. 2, pp. 1279–1286, 2019.

[5] B. Suger, B. Steder, and W. Burgard, "Traversability analysis for mobile robots in outdoor environments: A semi-supervised learning approach based on 3d-lidar data," in *2015 IEEE International Conference on Robotics and Automation (ICRA)*. IEEE, 2015, pp. 3941–3946.

[6] C. A. Brooks and K. Iagnemma, "Vibration-based terrain classification for planetary exploration rovers," *IEEE Transactions on Robotics*, vol. 21, no. 6, pp. 1185–1191, 2005.

[7] A. Valada and W. Burgard, "Deep spatiotemporal models for robust proprioceptive terrain classification," *The International Journal of Robotics Research*, vol. 36, no. 13-14, pp. 1521–1539, 2017.

[8] P. Giguere and G. Dudek, "A simple tactile probe for surface identification by mobile robots," *IEEE Transactions on Robotics*, vol. 27, no. 3, pp. 534–544, 2011.

[9] B. Sofman, E. Lin, J. A. Bagnell, J. Cole, N. Vandapel, and A. Stentz, "Improving robot navigation through self-supervised online learning," *Journal of Field Robotics*, vol. 23, no. 11-12, pp. 1059–1075, 2006.

[10] L. Wellhausen, A. Dosovitskiy, R. Ranftl, K. Walas, C. Cadena, and M. Hutter, "Where should i walk? predicting terrain properties from images via self-supervised learning," *IEEE Robotics and Automation Letters*, vol. 4, no. 2, pp. 1509–1516, 2019.

[11] M. A. Bekhti, Y. Kobayashi, and K. Matsumura, "Terrain traversability analysis using multi-sensor data correlation by a mobile robot," in *2014 IEEE/SICE International Symposium on System Integration*, pp. 615–620.

[12] H. Hauser, "Physical Reservoir Computing in Robotics," *Natural Computing Series*, pp. 169–190, 2021. [Online]. Available: https://link.springer.com/chapter/10.1007/978-981-13-1687-6_8

[13] M. Lukoševičius, H. Jaeger, and B. Schrauwen, "Reservoir computing trends," *KI-Künstliche Intelligenz*, vol. 26, no. 4, pp. 365–371, 2012.

[14] K. Nakajima, H. Hauser, T. Li, and R. Pfeifer, "Information processing via physical soft body," *Scientific reports*, vol. 5, no. 1, pp. 1–11, 2015.

[15] H. Hauser, A. J. Ijspeert, R. M. Füchslin, R. Pfeifer, and W. Maass, "Towards a theoretical foundation for morphological computation with compliant bodies," *Biological cybernetics*, vol. 105, no. 5, pp. 355–370, 2011.

[16] P. Childs, *Mechanical Design (3rd Edition)*. Butterworth-Heinemann, 2021.

[17] Z. Yu, S. H. Sadati, H. Wegiriya, P. Childs, and T. Nanayakkara, "A method to use nonlinear dynamics in a whisker sensor for terrain identification by mobile robots," in *2021 IEEE/RSJ International Conference on Intelligent Robots and Systems (IROS)*. IEEE, 2021, pp. 8437–8443.

[18] J. Zürn, W. Burgard, and A. Valada, "Self-supervised visual terrain classification from unsupervised acoustic feature learning," *IEEE Transactions on Robotics*, vol. 37, no. 2, pp. 466–481, 2020.